typeset using JPSJ.sty <ver.1.0b>

arXiv:cond-mat/9912482v1 [cond-mat.str-el] 30 Dec 1999

Ground State Properties of an $S = 1/2$ Distorted Diamond Chain

Takashi TONEGAWA*, Kiyomi OKAMOTO[1,**], Toshiya HIKIHARA[2], Yutaka TAKAHASHI[3], and Makoto KABURAGI[4]

Department of Physics, Faculty of Science, Kobe University, Rokkodai, Kobe 657-8501
[1]*Department of Physics, Tokyo Institute of Technology, Oh-Okayama, Meguro-ku, Tokyo 152-8551*
[2] *Division of Information and Media Science, Graduate School of Science and Technology, Kobe University, Rokkodai, Kobe 657-8501*
[3] *Division of Physics, Graduate School of Science and Technology, Kobe University, Rokkodai, Kobe 657-8501*
[4]*Department of Informatics, Faculty of Cross-Cultural Studies, Kobe University, Tsurukabuto, Kobe 657-8501*

(Received December 3, 1999)

We investigate the ground state properties of an $S = 1/2$ distorted diamond chain described by the Hamiltonian $\mathcal{H} = J_1 \sum_\ell \big\{ \big(\vec{S}_{3\ell-1} \cdot \vec{S}_{3\ell} + \vec{S}_{3\ell} \cdot \vec{S}_{3\ell+1}\big) + J_2 \vec{S}_{3\ell-2} \cdot \vec{S}_{3\ell-1} + J_3 \big(\vec{S}_{3\ell-2} \cdot \vec{S}_{3\ell} + \vec{S}_{3\ell} \cdot \vec{S}_{3\ell+2}\big) - H S^z_\ell \big\}$ $(J_1,\ J_2,\ J_3 \geq 0)$, which models well a trimerized $S = 1/2$ spin chain system $Cu_3Cl_6(H_2O)_2{\cdot}2H_8C_4SO_2$. Using an exact diagonalization method by means of the Lanczös technique, we determine the ground state phase diagram in the $H = 0$ case, composed of the dimerized, spin fluid, and ferrimagnetic phases. Performing a degenerate perturbation calculation, we analyze the phase boundary line between the latter two phases in the $J_2,\ J_3 \ll J_1$ limit, the result of which is in good agreement with the numerical result. We calculate, by the use of the density matrix renormalization group method, the ground state magnetization curve for the case (a) where $J_1 = 1.0$, $J_2 = 0.8$, and $J_3 = 0.5$, and the case (b) where $J_1 = 1.0$, $J_2 = 0.8$, and $J_3 = 0.3$. We find that in the case (b) the 2/3-plateau appears in addition to the 1/3-plateau which also appears in the case (a). The translational symmetry of the Hamiltonian $\mathcal{H}$ is spontaneously broken in the 2/3-plateau state as well as in the dimerized state.

KEYWORDS: $S = 1/2$ distorted diamond chain, $Cu_3Cl_6(H_2O)_2{\cdot}2H_8C_4SO_2$, ground state phase diagram, dimerized phase, spin fluid phase, ferrimagnetic phase, ground state magnetization curve, magnetization plateau, spontaneous symmetry breaking, exact diagonalization method, density matrix renormalization group method, method of level spectroscopy

§1. Introduction

In the past years a great deal of work has been devoted to the study of quantum spin systems with competing interactions. This has stemmed largely from their being systems which include two phenomena of great interest, frustration and quantum fluctuation. Recently, magnetic properties of a trimerized $S = 1/2$ spin chain system $Cu_3Cl_6(H_2O)_2{\cdot}2H_8C_4SO_2$ have been experimentally studied by Ishii, Tanaka, Hori, Uekusa, Ohashi, Tatani, Narumi, and Kindo.[1)] (See below for the discussion on the competition of the exchange interactions in this system.) They have measured the temperature dependence of the magnetic susceptibility and also the magnetization curve at sufficiently low temperatures. Their results clearly demonstrate that the ground state of this system is nonmagnetic and that there exists the energy gap with the magnitude of about 3.9 T or 5.2 K between the ground state and a first exited magnetic state. Furthermore, the result for the magnetization measurement shows that the so-called 1/3-plateau in the magnetization curve may start from about 58 T.

As has been discussed by Ishii *et al.*,[1)] the magnetic properties of $Cu_3Cl_6(H_2O)_2{\cdot}2H_8C_4SO_2$ can be well described by the following Hamiltonian $\mathcal{H}$, which is a sum of the exchange interaction term $\mathcal{H}_{\rm ex}$ and the Zeeman term $\mathcal{H}_{\rm Z}$:

$$\mathcal{H} = \mathcal{H}_{\rm ex} + \mathcal{H}_{\rm Z}\ , \tag{1.1a}$$

$$\begin{aligned} \mathcal{H}_{\rm ex} = J_1 \sum_{\ell=1}^{N/3} \big(\vec{S}_{3\ell-1} \cdot \vec{S}_{3\ell} + \vec{S}_{3\ell} \cdot \vec{S}_{3\ell+1}\big) \\ + J_2 \sum_{\ell=1}^{N/3} \vec{S}_{3\ell-2} \cdot \vec{S}_{3\ell-1} \\ + J_3 \sum_{\ell=1}^{N/3} \big(\vec{S}_{3\ell-2} \cdot \vec{S}_{3\ell} + \vec{S}_{3\ell} \cdot \vec{S}_{3\ell+2}\big)\ , \end{aligned} \tag{1.1b}$$

$$\mathcal{H}_{\rm Z} = -H \sum_{\ell=1}^{N} S^z_\ell\ , \tag{1.1c}$$

where $\vec{S}_\ell$ is the spin operator with the magnitude $S = 1/2$ for the Cu^{2+} ion located at the ℓth site, and periodic boundary conditions $\big(\vec{S}_{N+1} \equiv \vec{S}_1, \vec{S}_{N+2} \equiv \vec{S}_2\big)$ are imposed. In the following discussions, the total number N of spins is assumed to be a multiple of six. From the crystal structure and the lattice parameters of $Cu_3Cl_6(H_2O)_2{\cdot}2H_8C_4SO_2$, Ishii *et al.*,[1)] have inferred that three exchange constants, J_1, J_2, and J_3 are all antiferromagnetic (positive). Thus, the three interactions compete with each other. They have also inferred that

---

* tonegawa@kobe-u.ac.jp

** kokamoto@stat.phys.titech.ac.jp

J_1 is larger than J_2 and J_3. This means that the spins $\vec{S}_{3\ell-1}$, $\vec{S}_{3\ell}$, and $\vec{S}_{3\ell+1}$ form a trimer; J_1 is the intra-trimer exchange constant, and J_2 and J_3 are the inter-trimer ones. Schematical representations of the Hamiltonian $\mathcal{H}_{\rm ex}$ are given in Figs. 1(a) and 1(b). Referring to Fig. 1(a), we may call this model the 'distorted diamond chain model'.

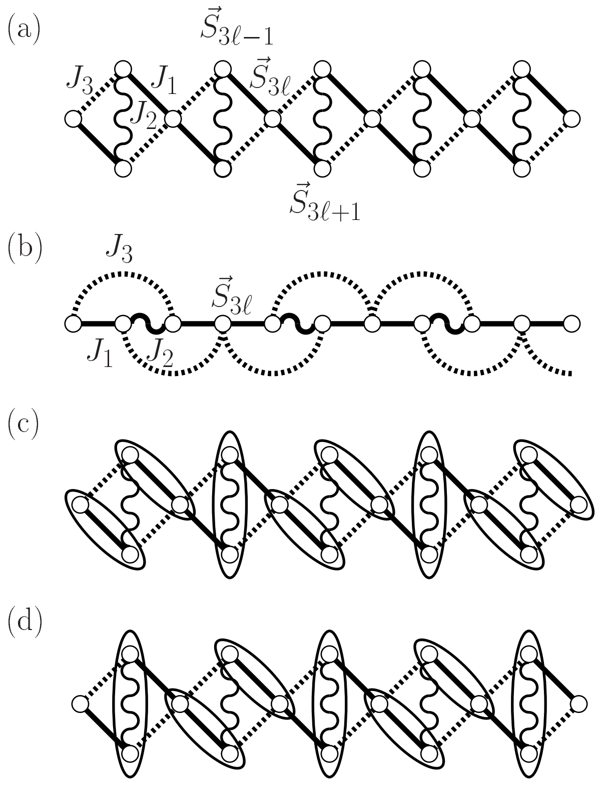

Fig. 1. (a) and (b) Two ways of representing schematically the Hamiltonian $\mathcal{H}_{\rm ex}$. (c) and (d) The two-fold degenerate dimerized (D) states. In (a) - (d), the open circles stand for the $S=1/2$ spins, and the solid, wavy, and dotted lines correspond to the J_1, J_2, and J_3 interactions, respectively. Two spins surrounded by an ellipse in (c) and (d) form a singlet dimer

In the present paper, we explore the ground-state properties of the distorted diamond chain, performing mainly numerical calculations based on the Lanczös method as well as the density matrix renormalization group (DMRG) method.[2,3] We focus our attention upon the ground state phase diagram in the case of zero external magnetic field ($H=0$) and the ground state magnetization curve. We treat the case where $J_1 \geq J_3$ and $J_2 \geq 0$, noting that the $J_1 < J_3$ case is equivalent to the $J_1 > J_3$ case by interchanging the role of J_1 and J_3.

Let us now discuss three special cases where $H=0$ is assumed. First, when $J_2=0$, we can readily show by the use of the Lieb-Mattis theorem[4] that the ground state is a ferrimagnetic (FRI) state where the magnitude $S_{\rm tot}$ of the total spin $\vec{S}_{\rm tot}=\sum_{\ell=1}^{N}\vec{S}_\ell$ $\bigl(\vec{S}_{\rm tot}^2=S_{\rm tot}(S_{\rm tot}+1)\bigr)$ is given by $S_{\rm tot}=N/6$. We note that this value is one third of that of the maximum (ferromagnetic) value, $N/2$. Second, when $J_3=0$, the system is reduced to the J_1-J_1-J_2 trimerized $S=1/2$ antiferromagnetic chain; in particular, if $J_1=J_2$, the $S=1/2$ uniform antiferromagnetic chain is obtained. Thus, the ground state is the spin fluid (SF) state with $S_{\rm tot}=0$, which has no excitation energy gap.[5]

Third, the case where $J_1=J_3$ has already been investigated by Takano, Kubo, and Sakamoto.[6] They have shown that the ground state is the FRI state with $S_{\rm tot}=N/6$, the tetramer-dimer (TD) state with $S_{\rm tot}=0$, or the dimer-monomer (DM) state with $S_{\rm tot}=0$, depending on whether $J_2/J_1<0.909$, $0.909<J_2/J_1<2$, or $2<J_2/J_1$. In the TD state, quadruplets $\vec{S}_{3\ell-3}$, $\vec{S}_{3\ell-2}$, $\vec{S}_{3\ell-1}$, and $\vec{S}_{3\ell}$ (or $\vec{S}_{3\ell}$, $\vec{S}_{3\ell+1}$, $\vec{S}_{3\ell+2}$, and $\vec{S}_{3\ell+3}$) of spins form singlet tetramers, and pairs $\vec{S}_{3\ell+1}$ and $\vec{S}_{3\ell+2}$ ($\vec{S}_{3\ell+4}$ and $\vec{S}_{3\ell+5}$) of spins, which we call J_2-pairs, singlet dimers. Thus, the TD state is two-fold degenerate. In the DM state, on the other hand, the J_2-pairs form singlet dimers, and the remaining monomer spins $\vec{S}_{3\ell}$ are free, which leads to $2^{N/3}$-fold degeneracy. These are schematically illustrated in Fig. 1 in ref. 6. The explicit expressions of the eigenfunctions and some physical quantities for both the TD and the DM state are given in Appendix. As has been shown by Takano *et al.*,[6] the commutation relation $\bigl[\mathcal{H}_{\rm ex},\ \bigl(\vec{S}_{3\ell+1}+\vec{S}_{3\ell+2}\bigr)^2\bigr]=0$ holds in the $J_1=J_3$ case. Therefore, each J_2-pair forms a singlet or a triplet. It is interesting to note that in the DM and FRI states, all the J_2-pairs form the singlets and the triplets, respectively, while in the TD state the singlet and triplet J_2-pairs are arranged alternatively.

In a recent paper,[7] Okamoto, Tonegawa, Takahashi, and Kaburagi have studied the ground state of the distorted diamond chain in the case of $H=0$, employing analytical methods based mainly on the bosonization technique and doing physical considerations. According to them, a tetramer in Takano *et al.*'s TD state is very peculiar to the $J_1=J_3$ case, and when $J_1>J_3$, the tetramer consisting of the spins, $\vec{S}_{3\ell-3}$, $\vec{S}_{3\ell-2}$, $\vec{S}_{3\ell-1}$, and $\vec{S}_{3\ell}$ is decomposed into two dimers, one of which consists of $\vec{S}_{3\ell-3}$ and $\vec{S}_{3\ell-2}$, and the other of $\vec{S}_{3\ell-2}$ and $\vec{S}_{3\ell-1}$. Thus, the TD state is a special case of the two-fold degenerate dimerized (D) state with $S_{\rm tot}=0$, shown in Figs. 1(c) and 1(d). The DM state is also peculiar to the $J_1=J_3$ case. When $J_1>J_3$, the monomer is no longer free and interacts with neighboring monomers through the dimer between them. Thus, the DM state is a special case of the SF state with $S_{\rm tot}=0$.

Summarizing these, Okamoto *et al.*[7] have concluded that the ground state phase diagram of the distorted diamond chain is composed of the D and SF phases plus the FRI phase which is stable at least when J_2 is sufficiently smaller than J_1 and J_3. They have also shown that the transition between the D and SF phases is of the Berezinskii-Kostelitz-Thouless (BKT) type, as in the case of the $S=1/2$ antiferromagnetic chain with uniform nearest and next-nearest neighbor interactions,[8] and have presented the ground state phase diagram determined numerically. In the region where the D state is the ground state, there exists a finite gap between the two-fold degenerate ground state and a first exited state. As can be seen from Figs. 1(c) and 1(d), the period of the translational symmetry of the D state is six, which is twice as large as that of the Hamiltonian $\mathcal{H}_{\rm ex}$. Thus, the spontaneous symmetry breaking occurs in the D ground state. This is consistent with the necessary condition for the appearance of the plateau in the ground state magnetization curve,

$$n(S-m) = \text{integer}\ , \tag{1.2}$$

obtained by Oshikawa, Yamanaka, and Affleck,[9] Here, n and m are, respectively, the period of translational symmetry of the plateau state and the average magnetization per site in the plateau, and S is the magnitude of spins in the system. (Note that $n=6$, $S=1/2$ and $m=0$ for the present ground D state in the $H=0$ case.)

In the present paper, we discuss the derivation of the ground state phase diagram in more detail. Furthermore, we discuss the ground state magnetization curve, as mentioned before.

§2. Ground State Phase Diagram in the $H=0$ Case

Let us denote, respectively, by $E^{(0)}(S_{\rm tot};\,N)$ and $E^{(1)}(S_{\rm tot};\,N)$ the lowest and second-lowest energy eigenvalues for a given set of $S_{\rm tot}$ and N of the Hamiltonian $\mathcal{H}_{\rm ex}$. We have calculated numerically these eigenvalues for finite size systems with $N=6$, 12, 18, and 24, employing the computer program package KOBEPACK/S[10] coded by one of the present authors (M. K.) by means of the Lanczös technique. Our calculation shows that, depending on the values of J_1, J_2, and J_3, only $E^{(0)}(0;\,N)$ or $E^{(0)}(N/6;\,N)$ becomes minimum among $E^{(0)}(S_{\rm tot};N)$'s for all values of $S_{\rm tot}(=0,\,1,\,\cdots,\,N/2)$. This is consistent with the fact that the ground state phase diagram is composed of the D, SF, and FRI phases,[7] as discussed in § 1.

The ground state phase is the FRI phase when $E^{(0)}(N/6;\,\infty) < E^{(0)}(0;\,\infty)$, and it is the D or the SF phase when $E^{(0)}(N/6;\,\infty) > E^{(0)}(0;\,\infty)$. We estimate the critical value $J_{i,{\rm c}}^{\rm FRI-0}$ of J_i ($i=1$ 2, or 3) between the former phase and one of the latter phases for a given set of the other two J's in the following way. We first calculate numerically the value $J_{i,{\rm c}}^{\rm FRI-0}(N)$ which satisfies

$$E^{(0)}(N/6;\,N) = E^{(0)}(0;\,N)\ . \tag{2.1}$$

Then, we estimate $J_{i,{\rm c}}^{\rm FRI-0}$ by fitting $J_{i,{\rm c}}^{\rm FRI-0}(N)$'s with 12, 18, and 24 to a quadratic function of $1/N^2$, that is,

$$J_{i,{\rm c}}^{\rm FRI-0}(N) = J_{i,{\rm c}}^{\rm FRI-0} + \frac{a}{N^2} + \frac{b}{N^4}\ , \tag{2.2}$$

where a and b are numerical constants.

On the other hand, in order to estimate the critical value $J_{i,{\rm c}}^{\rm D-SF}$ between the D and SF phases, we employ the method of level spectroscopy,[8,11] which has been successfully applied to estimate numerically the BKT critical points in many cases. The procedure of the method is as follows. (For the physical interpretation of this procedure the reader is referred, for example, to ref. 7.) First, we introduce the singlet-singlet energy gap $\Delta_{\rm ss}(N)$ and the singlet-triplet energy gap $\Delta_{\rm ss}(N)$ for the finite-N system defined by

$$\Delta_{\rm ss}(N) = E^{(1)}(0;\,N) - E^{(0)}(0;\,N)\ , \tag{2.3a}$$

$$\Delta_{\rm st}(N) = E^{(0)}(1;\,N) - E^{(0)}(0;\,N)\ , \tag{2.3b}$$

where $E^{(0)}(0;\,N)$ is nothing but the ground state energy. Then, we calculate the value $J_{i,{\rm c}}^{\rm D-SF}(N)$ satisfying

$$\Delta_{\rm ss}(N) = \Delta_{\rm st}(N)\ . \tag{2.4}$$

Finally, we extrapolate the results $J_{i,{\rm c}}^{\rm D-SF}(N)$'s to $N\to\infty$ by the use of a polynomial of $1/N^2$ to estimate $J_{i,{\rm c}}^{\rm D-SF}$. In the practical calculations we have performed this extrapolation by using the values of $J_{i,{\rm c}}^{\rm D-SF}(N)$'s with 12, 18, and 24 and the formula,

$$J_{i,{\rm c}}^{\rm D-SF}(N) = J_{i,{\rm c}}^{\rm D-SF} + \frac{a'}{N^2} + \frac{b'}{N^4} \tag{2.5}$$

with numerical constants a' and b'.

We can obtain the ground state phase diagram on a exchange constant parameter plane by plotting the estimated critical points and by connecting them as smoothly as possible. The results are depicted in Figs. 2(a) and 2(b), which show, respectively, the phase diagram on the J_3 versus J_2 plane with J_1 fixed at $J_1=1$ and that on the J_3 versus J_1 plane with $J_1=1$; note that the former is a replot of Fig. 9 in ref. 7. In these phase diagrams the case where $J_1<J_3$ is included to make them more complete.

The phase transition between the FRI phase and the D or the SF phase is, of course, of first order. Furthermore, when $J_1=J_3$, the transition between the D and SF phases, or equivalently, that between Takano *et al.*'s TD and DM phases, at $J_2/J_1=2$ is also of first order. As is shown in Appendix, the ground state energy $\varepsilon_{\rm g}(N)$ per site for $0.909<J_2/J_1<2$ and that for the $2<J_2/J_1$ case are, respectively, given by $\varepsilon_{\rm g}(N) = E_{\rm TD}(N)/N = -(4J_1+J_2)/12$ and $\varepsilon_{\rm g}(N) = E_{\rm DM}(N)/N = -J_2/4$, and therefore, plotting $\partial\varepsilon_{\rm g}(N)/\partial J_1$ as a function of J_1, we have a discontinuity at $J_1=J_2/2$.

We assert, for the following reasons, that the first order phase transition is peculiar only to the above two cases in the present system. Let us first give a physical consideration. It is well known that the ground state of the $S=1/2$ chain with uniform, antiferromagnetic nearest and next-nearest neighbor interactions is a two-fold degenerate dimerized state which is essentially equivalent to those shown by Figs. 1(c) and 1(d), as far as the latter interaction is sufficiently larger than the former one.[8,12,13] If a bond alternation is introduced in the nearest neighbor interaction as a perturbation, the degeneracy of the ground state is lifted, and one of the dimerized state or the other becomes the ground state depending upon the value of a bond alternation parameter. Thus, sweeping this parameter, we have the first order transition in the ground state at the uniform point. In fact, the first order transition has been observed, for example, in the ground state of a generalized $S=1/2$ ladder with additional exchange interactions on diagonal bonds,[14] which has bond alternating nearest neighbor interactions when represented in a one-dimensional chain scheme like Fig. 1(b). In the present distorted diamond chain, on the other hand, we have no bond alternation, but have a bond trimerization in the nearest

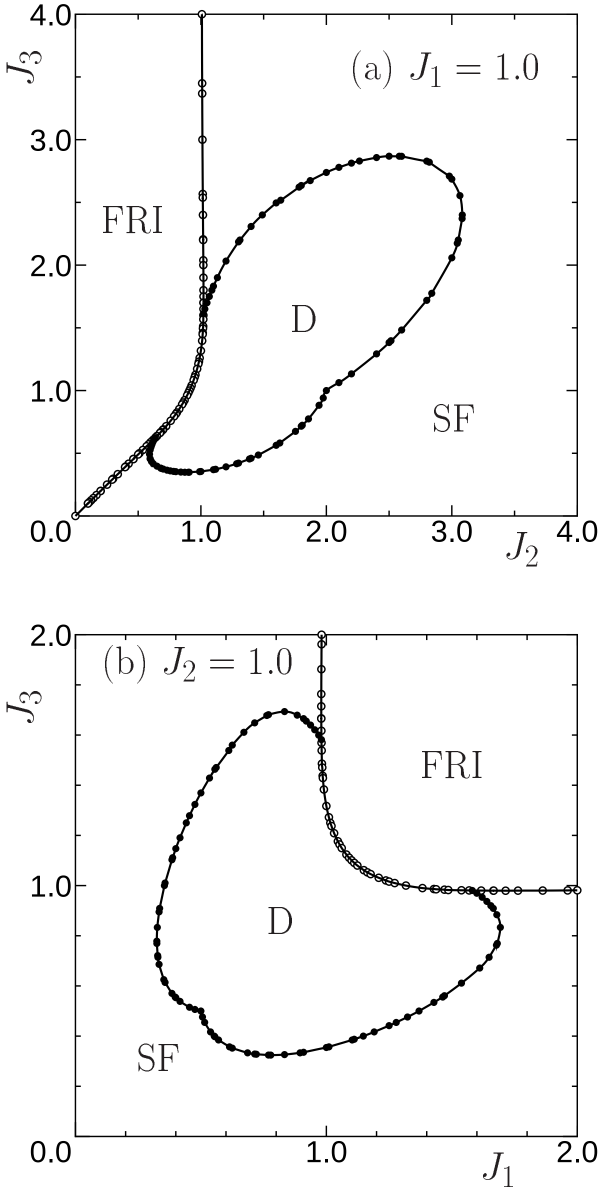

Fig. 2. Ground state phase diagrams (a) on the J_3 versus J_2 plane with $J_1 = 1$ and (b) on the J_3 versus J_1 plane with $J_1 = 1$. The phase diagrams are composed of the dimerized (D), spin fluid (SF), and ferrimagnetic (FRI) phases.

neighbor interaction [see Fig. 1(d)] which never lifts a two-fold degeneracy in the D ground state. Thus, no first order transition occurs in the ground state of the present chain, except for the two peculiar cases stated above.

In order to supplement the above reason discussed physically, we have calculated numerically the J_1-dependence of $\partial\varepsilon_{\rm g}(N)/\partial J_1$ with $N = 6$, 12, 18, and 24 for the $J_2 = 1$ and $J_3/J_1 = 0.999$ case, for which the D-SF critical point is given by $J_{1,{\rm c}}^{\rm D-SF} \sim 0.5002$ according to the phase diagram shown in Fig. 2(b). The result is plotted in Fig. 3, together with that for the $J_2 = 1$ and $J_3/J_1 = 1$ case mentioned above. This figure demonstrates clearly that $\partial\varepsilon_{\rm g}(N)/\partial J_1$ for the $J_2 = 1$ and $J_3/J_1 = 0.999$ case have no anomaly around $J_1 = 0.5$. This result suggests that we have no first order transition in the $J_1 < J_3$ case (and also in the $J_1 > J_3$ case) except for the FRI-D transition.

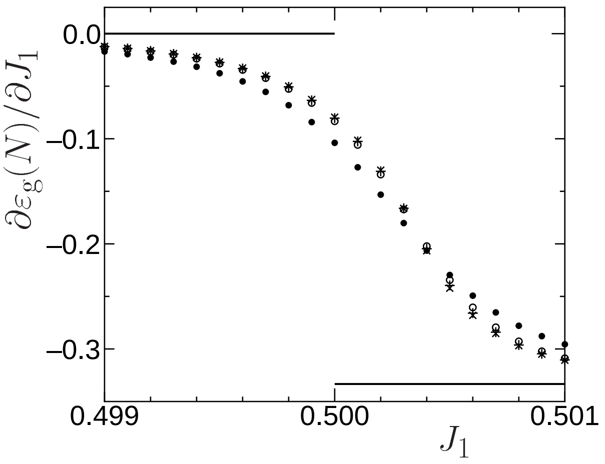

Fig. 3. Plot versus J_1 of $\partial\varepsilon_{\rm g}(N)/\partial J_1$ with $N = 6$ (closed circles), 12 (open circles), 18 (pluses), and 24 (crosses) for $J_2 = 1$ and $J_3/J_1 = 0.999$, together with that (solid lines) for $J_2 = 1$ and $J_3/J_1 = 1$.

§3. Ground State Magnetization Curve

We have calculated the ground state magnetization curve of the present system, using the DMRG method proposed originally by White.[2)] Here, we describe briefly the procedure for our DMRG calculation. We employ the finite system algorithm[3)] as improved by White,[15)] which reduces substantially the required computational time. The maximum number of block states we keep in the calculation is $m_{\rm max} = 100$, which leads to the truncation error of the order of 10^{-8}. Comparing the calculated results for the cases where $m = 70$ and $m = 100$ block states are kept, we may conclude that the results for $m = 100$ are within an accuracy of roughly $10^{-4} \sim 10^{-5}$. Thus, we adopt these results as our final results without carrying out any m-extrapolation. We assume open boundary conditions for the Hamiltonian $\mathcal{H}_{\rm ex}$, subtracting the two terms, $J_1\,\vec{S}_N \cdot \vec{S}_{N+1} \big(\equiv J_1 \vec{S}_N \cdot \vec{S}_1\big)$ and $J_3\,\vec{S}_N \cdot \vec{S}_{N+2} \big(\equiv J_3 \vec{S}_N \cdot \vec{S}_2\big)$, from the expression of eq. (1.1b). This is because, as is well known, open boundary conditions make the DMRG method work more effectively. It should be noted that these boundary conditions lead to an open chain which has no inversion symmetry with respect to its center.

For finite size systems with up to $N = 96$ spins, we have calculated the lowest energy eigenvalue $\bar{E}^{(0)}(M;\,N)$ of $\mathcal{H}_{\rm ex}$ within the subspace determined by the value M of the z-component of $\vec{S}_{\rm tot}$. Once the values of $\bar{E}^{(0)}(M;\,N)$ for nonnegative M's ($M = 0,\,1,\,\cdots,\,N/2$) are known, the ground state magnetization curve can be obtained by plotting as a function of H the average magnetization

$m(N)(=M/N)$ per site determined from

$$m(N) = \begin{cases} 0 & \left(\text{when } \Delta\bar{E}_q^{(0)}(M, M-q;\, N) > H\right), \\ \dfrac{\max\left[\, M \,\middle|\, \Delta\bar{E}_q^{(0)}(M,M-q;\, N)<H \,\right]}{N} & (\text{otherwise}), \end{cases} \tag{3.1}$$

with $M=1,\,2,\,\cdots,\,N/2$, and $q=1,\,2,\,\cdots,\,M$, where

$$\Delta\bar{E}_q^{(0)}(M, M-q;\, N) = \frac{\bar{E}^{(0)}(M;\, N) - \bar{E}^{(0)}(M-q;\, N)}{q}\,. \tag{3.2}$$

It is noted that $m(N)=0$ when $0 \le H \le H_0(N)$, where $H_0(N)=\min\{\Delta\bar{E}_q^{(0)}(q, 0;\, N)\}$, and the saturation field $H_{\rm s}(N)$ is given by $H_{\rm s}(N)=\max\{\Delta\bar{E}_q^{(0)}(\frac{N}{2}, \frac{N}{2}-1;\, N)\}$. The resulting magnetization curve is a stepwisely increasing function of H. In particular, when the ground state in the case of $H=0$ is the $S_{\rm tot}=0$ state and the competition among the three interactions is not too strong, the magnetization curve has $N/2$ steps, starting from $m(N)=0$ and ending at $m(N)=1/2$; at each step $m(N)$ increases by $1/N$.[16] Then, $H_0(N) = \Delta\bar{E}_1^{(0)}(1, 0;\, N) = \Delta_{\rm st}(N)$, and $H_{\rm s}(N) = \Delta\bar{E}_1^{(0)}(M, M-1; N)$. Following Bonner and Fisher's pioneering work,[17] we may obtain, except for plateau regions, a satisfactorily good approximation to the magnetization curve in the thermodynamic $(N\to\infty)$ limit by drawing a smooth curve through the midpoints of the steps in the finite size results.

Table I. Numerical values of $H_0(N)/H_{\rm s}(N)$, $H_{1/3,{\rm l}}(N)/H_{\rm s}(N)$, $H_{1/3,{\rm h}}(N)/H_{\rm s}(N)$, $H_{2/3,{\rm l}}(N)/H_{\rm s}(N)$, and $H_{2/3,{\rm h}}(N)/H_{\rm s}(N)$ estimated in the cases (a) and (b). Note that the figures in the parentheses for the $N\to\infty$ values show errors in the last digit.

(a) the case (a) where $J_1=1.0$, $J_2=0.8$, and $J_3=0.5$.

	$N=48$	$N=72$	$N=96$	$N\to\infty$
$\frac{H_0(N)}{H_{\rm s}(N)}$	0.024525	0.016736	0.012795	0.0033 (5)
$\frac{H_{1/3,{\rm l}}(N)}{H_{\rm s}(N)}$	0.160260	0.160875	0.161043	0.1612 (1)
$\frac{H_{1/3,{\rm h}}(N)}{H_{\rm s}(N)}$	0.702154	0.699845	0.699090	0.6982 (1)

(b) the case (b) where $J_1=1.0$, $J_2=0.8$, and $J_3=0.3$.

	$N=48$	$N=72$	$N=96$	$N\to\infty$
$\frac{H_0(N)}{H_{\rm s}(N)}$	0.031482	0.021075	0.015841	0.0
$\frac{H_{1/3,{\rm l}}(N)}{H_{\rm s}(N)}$	0.312021	0.314803	0.315499	0.3162 (1)
$\frac{H_{1/3,{\rm h}}(N)}{H_{\rm s}(N)}$	0.842373	0.841792	0.841618	0.8414 (1)
$\frac{H_{2/3,{\rm l}}(N)}{H_{\rm s}(N)}$	0.902840	0.905461	0.906667	0.9084 (1)
$\frac{H_{2/3,{\rm h}}(N)}{H_{\rm s}(N)}$	0.944329	0.942955	0.942391	0.9416 (1)

Figure 4 shows the magnetization curves calculated for $N=96$; Figs. 4(a) and 4(b) are, respectively, for the case (a) where $J_1 = 1.0$, $J_2 = 0.8$, and $J_3 = 0.5$, and for the case (b) where $J_1 = 1.0$, $J_2 = 0.8$, and $J_3 = 0.3$. In each case, we have a 1/3-plateau, and moreover, in the case (b), we have a 2/3-plateau in addition to this. We denote the highest and lowest values of H giving the p-plateau ($p=1/3$, 2/3) by $H_{p,{\rm h}}(N)$ and $H_{p,{\rm l}}(N)$, respectively. We have calculated these as well as $H_0(N)$ and $H_{\rm s}(N)$ also for $N=72$ and 48 in the cases (a) and (b), and have extrapolated the results to $N\to\infty$ to estimate the values in the thermodynamic limit. The results are tabulated in Table I. We see from this Table that, except for $H_0(N)$, the finite size results for $N=96$ give good approximations to the results in the thermodynamic limit.

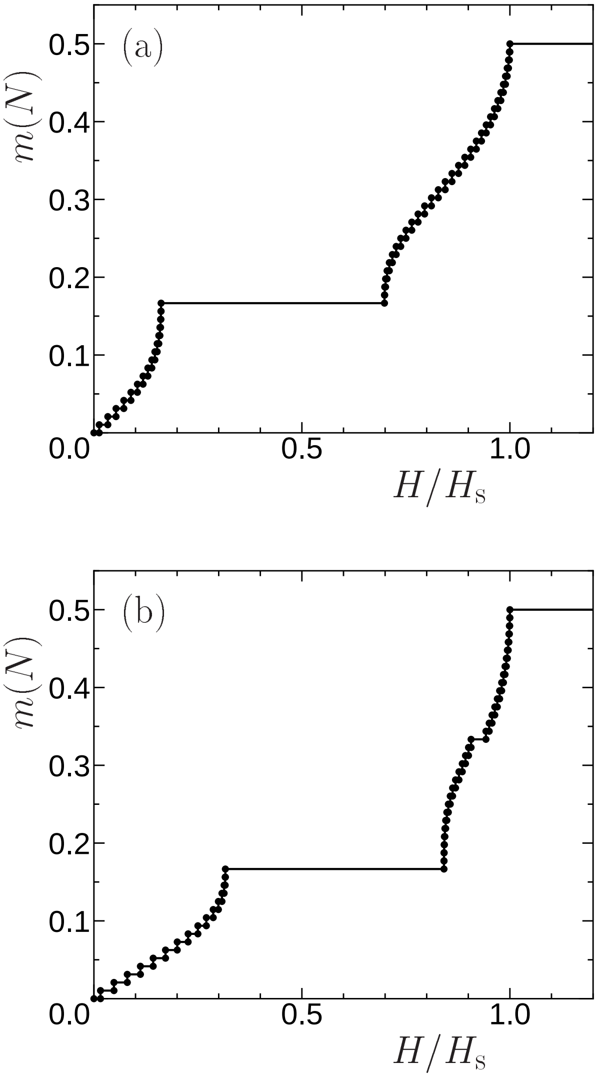

Fig. 4. Ground state magnetization curves calculated for $N=96$ (a) in the case (a) where $J_1=1.0$, $J_2=0.8$, and $J_3=0.5$ and (b) in the case (b) where $J_1=1.0$, $J_2=0.8$, and $J_3=0.3$.

The 1/3-plateau state is essentially the same as the ferrimagnetic state which becomes the ground state when $J_3 > J_{3,{\rm c}}^{\rm FRI-0} \sim 0.813$ in the $J_1=1.0$, $J_2=0.8$, and $H=0$ case. On the other hand, we see from eq. (1.2) that the periodicity n of the 2/3-plateau state should be a multiple of six, since $S=1/2$ and $M=1/3$. In order to check this fact, we have calculated, by means of the DMRG method, the ℓ-dependence of the expectation value $m(\ell;\, N)$ of S_ℓ^z for the 2/3-plateau state in the case (b). The results for $N=96$ depicted in Fig. 5 clearly demonstrates that $n=6$ for this state, which means that the translational symmetry is spontaneously broken also

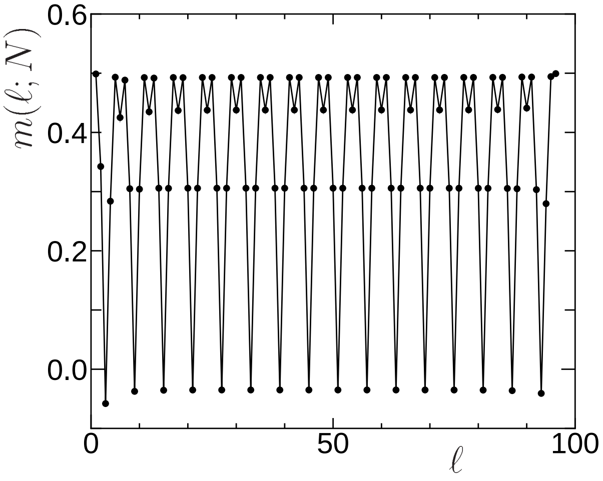

Fig. 5. Plot versus ℓ of $m(\ell;\, N)$ with $N=96$ for the 2/3-plateau state in the case (b) where $J_1=1.0$, $J_2=0.8$, and $J_3=0.3$. Solid lines are guides to the eye.

in this state as in the D state. Thus, the mechanism for the appearance of the 2/3-plateau in the present case is considered to be the same as that, which has been clarified by Totsuka,[18] for the appearance of the 1/2-plateau in the ground state magnetization curve of the $S=1/2$ antiferromagetic chain with bond alternating nearest and uniform next-nearest neighbor interactions.[19] Based on this mechanism, we can determine, by using the method of level spectroscopy,[8, 11] the region, where the 2/3-plateau appears, of J_i for a given set of the other two J'. Leaving the details of this investigation for a forthcoming paper, we only mention here that, according our preliminary result, the 2/3-plateau appears when $0.169 \lesssim J_3 \lesssim 0.375$ in the $J_1=1.0$ and $J_2=0.8$ case.

§4. Concluding Remarks and Discussion

We have explored the ground state properties of an $S=1/2$ distorted diamond chain described by the Hamiltonian $\mathcal{H}$ [see eqs. (1.1a)-(1.1c)], which models well a trimerized $S=1/2$ spin chain system $\mathrm{Cu_3Cl_6(H_2O)_2{\cdot}2H_8C_4SO_2}$. Using an exact diagonalization method by means of the Lanczös technique, we have determined the ground state phase diagram in the $H=0$ case [Figs. 2(a) and 2(b)], composed of the D, SF, and FRI phases. As has been mentioned in § 1, the ground state of $\mathrm{Cu_3Cl_6(H_2O)_2{\cdot}2H_8C_4SO_2}$ is nonmagnetic with a relatively small but finite energy gap. Furthermore, the three exchange constants, J_1, J_2, and J_3, in this system satisfy $J_1 > J_2,\ J_3 > 0$. From these facts together with the obtained phase diagram shown in Figs. 2(a), we may anticipate that in $\mathrm{Cu_3Cl_6(H_2O)_2{\cdot}2H_8C_4SO_2}$ the values of J_2/J_1 and J_3/J_1 are in the region of $0.7 \lesssim J_2/J_1 \lesssim 0.9$ and $0.45 \lesssim J_3/J_1 \lesssim 0.65$. We have also calculated, by the use of the density matrix renormalization group method, the ground state magnetization curve for the case (a) where $J_1=1.0$, $J_2=0.8$, and $J_3=0.5$ [Fig.4 (a)], and the case (b) where $J_1=1.0$, $J_2=0.8$, and $J_3=0.3$ [Fig. 4(b)]. We have found that in the case (b) the 2/3-plateau appears in addition to the 1/3-plateau which also appears in the case (a), and have clarified that the translational symmetry of the Hamiltonian $\mathcal{H}_{\rm ex}$ is spontaneously broken in the 2/3-plateau state.

Figure 2(a) demonstrates that the boundary line between FRI and SF phases in the limit of $0 \le J_2 \ll J_1$ and $0 \le J_3 \ll J_1$ is approximately given by $J_2=J_3$. This can be understood analytically by performing a degenerate perturbation calculation around the truncation point $J_2=J_3=0$ in the following way. The unperturbed Hamiltonian $\mathcal{H}_0$ is given by the sum of the Hamiltonian h_ℓ for the ℓth trimer consisting of $\vec{S}_{3\ell-1}$, $\vec{S}_{3\ell}$, and $\vec{S}_{3\ell+1}$:

$$\mathcal{H}_0 = \sum_{\ell=1}^{N/3} h_\ell\,, \tag{4.1a}$$

$$h_\ell = \vec{S}_{3\ell-1}\cdot\vec{S}_{3\ell} + \vec{S}_{3\ell}\cdot\vec{S}_{3\ell+1}\,, \tag{4.1b}$$

where the value of J_1 is taken to be $J_1=1.0$ as the unit of energy. The eigenfunctions, $\phi_\ell^{(1)}$ and ϕ_ℓ^2, of the lowest energy states of h_ℓ, which are two-fold degenerate, are expressed, by the use of α_ℓ and β_ℓ representing, respectively, the $S_\ell^z=1/2$ and $S_\ell^z=-1/2$ single spin states, as

$$\phi_\ell^{(1)} = \frac{1}{\sqrt{6}}\bigl\{|\alpha_{3\ell-1}\alpha_{3\ell}\beta_{3\ell+1}\rangle - 2\,|\alpha_{3\ell-1}\beta_{3\ell}\alpha_{3\ell+1}\rangle + |\beta_{3\ell-1}\alpha_{3\ell}\alpha_{3\ell+1}\rangle\bigr\}\,, \tag{4.2a}$$

$$\phi_\ell^{(2)} = \frac{1}{\sqrt{6}}\bigl\{|\beta_{3\ell-1}\beta_{3\ell}\alpha_{3\ell+1}\rangle - 2\,|\beta_{3\ell-1}\alpha_{3\ell}\beta_{3\ell+1}\rangle + |\alpha_{3\ell-1}\beta_{3\ell}\beta_{3\ell+1}\rangle\bigr\}\,. \tag{4.2b}$$

Restricting only to these two eigenfunctions, we can represent $\vec{S}_{3\ell-1}$, $\vec{S}_{3\ell}$, and $\vec{S}_{3\ell+1}$ in terms of the pseudo $S=1/2$ operator $\vec{T}_\ell$ associated with the ℓth trimer:

$$S_{3\ell-1}^{\pm} = -\frac{2}{3}T_\ell^{\pm}\,, \qquad S_{3\ell-1}^{z} = \frac{2}{3}T_\ell^{z}\,, \tag{4.3a}$$

$$S_{3\ell}^{\pm} = \frac{1}{3}T_\ell^{\pm}\,, \qquad S_{3\ell}^{z} = -\frac{1}{3}T_\ell^{z}\,, \tag{4.3b}$$

$$S_{3\ell+1}^{\pm} = -\frac{2}{3}T_\ell^{\pm}\,, \qquad S_{3\ell+1}^{z} = \frac{2}{3}T_\ell^{z}\,, \tag{4.3c}$$

where the $T_\ell^z=1/2$ and $T_\ell^z=-1/2$ states correspond to $\phi_\ell^{(1)}$ and ϕ_ℓ^2, respectively. Substituting eqs. (4.3a)-(4.3c) into the second (J_2) and third (J_3) terms in the right-hand side of eq. (1.1b) leads to the following effective Hamiltonian $\mathcal{H}_{\rm eff}$:

$$\mathcal{H}_{\rm eff} = \frac{4}{9}\,(J_2 - J_3)\sum_{\ell=1}^{N/3}\vec{T}_\ell\cdot\vec{T}_{\ell+1} \tag{4.4}$$

with $\vec{T}_{(N/3)+1} \equiv \vec{T}_1$. We see from this equation that the ground state of the pseudo $\vec{T}_\ell$ spin system is the ferromagnetic or the SF state depending upon whether $J_2 > J_3$ or $J_2 < J_3$, the former and the latter corresponding, respectively, to the FRI and SF states in the original $\vec{S}_\ell$ spin system. Thus, it is shown that the $J_2=J_3$ line yields the boundary line between FRI and SF phases in the limit of $0 \le J_2 \ll J_1$ and $0 \le J_3 \ll J_1$.

Acknowledgments

We would like to thank Professors H.-J. Mikeska, K. Takano, K. Kubo, and H. Tanaka for valuable discussions. We are also thankful to the Supercomputer Center, Institute for Solid State Physics, University of Tokyo, the Computer Center, Tohoku University, and the Computer Room, Yukawa Institute for Theoretical Physics, Kyoto University for computational facilities. The present work has been supported in part by a Grant-in-Aid for Scientific Research (C) from the Ministry of Education, Science, Sports and Culture.

Appendix

Here, we discuss the $J_1=J_3$ case.[6] Let us introduce the following states:

$$\begin{aligned}
&[\,\ell,\,\ell+1,\,\ell+2,\,\ell+3\,]\\
&\quad=\frac{1}{\sqrt{12}}\big\{|\alpha_\ell\alpha_{\ell+1}\beta_{\ell+2}\beta_{\ell+3}\rangle+|\beta_\ell\beta_{\ell+1}\alpha_{\ell+2}\alpha_{\ell+3}\rangle\\
&\qquad+|\alpha_\ell\beta_{\ell+1}\alpha_{\ell+2}\beta_{\ell+3}\rangle+|\beta_\ell\alpha_{\ell+1}\beta_{\ell+2}\alpha_{\ell+3}\rangle\\
&\qquad-2\,|\alpha_\ell\beta_{\ell+1}\beta_{\ell+2}\alpha_{\ell+3}\rangle-2\,|\beta_\ell\alpha_{\ell+1}\alpha_{\ell+2}\beta_{\ell+3}\rangle\big\}\ ,
\end{aligned}\tag{A·1a}$$

$$[\,\ell,\,\ell+1\,]=\frac{1}{\sqrt{2}}\big\{|\alpha_\ell\beta_{\ell+1}\rangle-|\beta_\ell\alpha_{\ell+1}\rangle\big\}\ ,\tag{A·1b}$$

$$[\,\ell\,]=|\alpha_\ell\rangle \qquad \text{or} \qquad |\beta_\ell\rangle\ .\tag{A·1c}$$

Then, the eigenfunctions $\Phi^{\pm}_{\rm TD}(N)$ of the TD state for the finite-N system is given by

$$\Phi^{\pm}_{\rm TD}(N)=\frac{1}{\sqrt{2}}\big\{\Phi^{(1)}_{\rm TD}(N)\pm\Phi^{(2)}_{\rm TD}(N)\big\}\tag{A·2}$$

with

$$\begin{aligned}
&\Phi^{(1)}_{\rm TD}(N)\\
&\quad=[\,1,\,2\,]\,[\,3,\,4,\,5,\,6\,]\cdots\\
&\qquad[\,N-5,\,N-4\,]\,[\,N-3,\,N-2,\,N-1,\,N\,]\ ,
\end{aligned}\tag{A·3a}$$

$$\begin{aligned}
&\Phi^{(2)}_{\rm TD}(N)\\
&\quad=[\,N,\,1,\,2,\,3\,]\,[\,4,\,5\,]\cdots\\
&\qquad[\,N-6,\,N-5\,]\,[\,N-4,\,N-3,\,N-2,\,N-1\,]\ .
\end{aligned}\tag{A·3b}$$

Note here that $\langle\Phi^{(1)}_{\rm TD}(N)|\Phi^{(2)}_{\rm TD}(N)\rangle=0$. On the other hand, the eigenfunction $\Phi_{\rm DM}(N)$ of the DM state for the finite-N system is

$$\Phi_{\rm DM}(N)=[\,1,\,2\,]\,[\,3\,]\cdots[\,N-3,\,N-2\,]\,[\,N\,]\ .\tag{A·4}$$

It is easy to show that the energies of the TD and DM states for the finite-N system are given, respectively, by $E_{\rm TD}(N)=-\frac{N}{12}(4J_1+J_2)$ and $E_{\rm DM}(N)=-\frac{N}{4}J_2$. We note that $E_{\rm DM}(N)$ is the total energy of $\frac{N}{3}$ independent singlet dimers mentioned in § 1, while $E_{\rm TD}(N)$ is the total energy of $\frac{N}{6}$ independent singlet tetramers plus that of $\frac{N}{6}$ independent singlet dimers. Furthermore, it is also straightforward to calculate the spin pair correlation functions in the TD and DM states, defined, respectively, by

$$\omega_{\rm TD}(\ell,\ell';\,N)=\langle\Phi^{\pm}_{\rm TD}(N)|\vec{S}_\ell\cdot\vec{S}_{\ell'}|\Phi^{\pm}_{\rm TD}(N)\rangle\ ,\tag{A·5a}$$

$$\omega_{\rm DM}(\ell,\ell';\,N)=\langle\Phi^{\pm}_{\rm DM}(N)|\vec{S}_\ell\cdot\vec{S}_{\ell'}|\Phi^{\pm}_{\rm DM}(N)\rangle\ .\tag{A·5b}$$

When $N=12,\,18,\,\cdots$, the function $\omega_{\rm TD}(\ell,\ell';\,N)$ for $\ell\leq\ell'$[20] takes nonzero values independently of N only in the following cases:

$$\omega_{\rm TD}(\ell,\ell;\,N)=\frac{3}{4}\ ,\tag{A·6a}$$

$$\begin{aligned}
\omega_{\rm TD}(3\ell-2,3\ell;\,N)&=\omega_{\rm TD}(3\ell,3\ell+2;\,N)\\
&=-\frac{1}{12}\ ,
\end{aligned}\tag{A·6b}$$

$$\begin{aligned}
\omega_{\rm TD}(3\ell-1,3\ell;\,N)&=\omega_{\rm TD}(3\ell,3\ell+1;\,N)\\
&=-\frac{1}{12}\ ,
\end{aligned}\tag{A·6c}$$

$$\omega_{\rm TD}(3\ell+1,3\ell+2;\,N)=-\frac{1}{12}\ ,\tag{A·6d}$$

$$\omega_{\rm TD}(3\ell,3\ell+3;\,N)=\frac{1}{24}\ .\tag{A·6e}$$

On the other hand, the nonzero values of $\omega_{\rm DM}(\ell,\ell';\,N)$ for $\ell\leq\ell'$[20] are

$$\omega_{\rm DM}(\ell,\ell;\,N)=\frac{3}{4}\ ,\tag{A·7a}$$

$$\omega_{\rm DM}(3\ell+1,3\ell+2;\,N)=-\frac{3}{4}\ ,\tag{A·7b}$$

which are independent of $N(=6,\,12,\,18,\,\cdots)$.

---

1) M. Ishii, H. Tanaka, M. Hori, Y. Uekusa, Y. Ohashi, K. Tatani, Y. Narumi and K. Kindo: preprint.
2) S. R. White: Phys. Rev. Lett. **69** (1992) 2863.
3) S. R. White: Phys. Rev. B **48** (1993) 10345.
4) E. Lieb and D. Mattis: J. Math. Phys. **3** (1962) 749.
5) K. Okamoto and A. Kitzawa: J. Phys. A: Math. Gen. **32** (1999) 4601, and references therein.
6) K. Takano, K. Kubo and H. Sakamoto: J. Phys.: Condens. Matter **8** (1996) 6405.
7) K. Okamoto, T. Tonegawa, Y. Takahashi and M. Kaburagi: to appear in J. Phys.: Condens. Matter (cond-mat/9907440).
8) K. Okamoto and K. Nomura: Phys. Lett. A **169** (1992) 433.
9) M. Oshikawa, M. Yamanaka and I. Affleck: Phys. Rev. Lett. **78** (1997) 1084.
10) The algorithm used in the computer program package KOBEPACK/S has been discussed by M. Kaburagi, T. Tonegawa and T. Nishino [*Computational Approaches in Condensed Matter Physics*, Springer Proc. Phys., ed. S. Miyashita, M. Imada and H. Takayama (Springer, Berlin, 1992) p. 179].
11) K. Nomura: J. Phys. A: Math. Gen. **28** (1995) 5451.
12) C. K. Majumdar and D. K. Ghosh: J. Math. Phys. **10** (1969) 1399.
13) T. Tonegawa and I. Harada: J. Phys. Soc. Jpn. **56** (1987) 2153.
14) A. K. Kolezhuk and H.-J. Mikeska: Int. J. Mod. Phys. B **12** (1998) 2325.
15) S. R. White: Phys. Rev. Lett. **77** (1996) 3633.
16) When the ground state in the case of $H=0$ is the $S_{\rm tot}=N/6$ (ferrimagnetic) state, the magnetization curve starts, of course, from $m(N)=N/6$, and when the competition among the three interactions is sufficiently strong, some of the $N/2$ steps may be skipped.
17) J. C. Bonner and M. E. Fisher: Phys. Rev. **135** (1964) A640.
18) K. Totsuka: Phys. Rev. B **57** (1998) 3454.

19) T. Tonegawa, T. Nishida and M. Kaburagi: Physica B **246-247** (1998) 368.
20) Of course, the relations $\omega_{\rm TD}(\ell,\ell';N)=\omega_{\rm TD}(\ell',\ell;N)$ and $\omega_{\rm DM}(\ell,\ell';N)=\omega_{\rm DM}(\ell',\ell;N)$ hold.